Eur. Phys. J. D **42**, 203–210 (2007)
DOI: 10.1140/epjd/e2007-00029-5

THE EUROPEAN PHYSICAL JOURNAL D

Generalized Kolbenstvedt model for electron impact ionization of K-, L- and M-shell atoms

A.K.F. Haque[1], M.A. Uddin[1,a], M.A.R. Patoary[1], A.K. Basak[1], M.R. Talukder[2], B.C. Saha[3], K.R. Karim[4], and F.B. Malik[5,6]

[1] Department of Physics, University of Rajshahi, Rajshahi 6205, Bangladesh
[2] Department of Applied Physics & Electronic Engineering, University of Rajshahi, Rajshahi 6205, Bangladesh
[3] Department of Physics, Florida A&M University, Tallahassee, Florida 32307, USA
[4] Department of Physics, Department of Physics, Illinois State University, Normal, IL 61790, USA
[5] Department of Physics, Southern Illinois University, Carbondale, IL 62901, USA
[6] Department of Physics, Washington University, St. Louis, MO 63130, USA

Received 21 December 2006 / Received in final form 22 January 2007
Published online 14 February 2007 –

Abstract. The recently modified Kolbenstvedt (MKLV) model [Eur. Phys. J. D **37**, 361 (2006)], developed for electron impact ionization (EII) of the K-shell atomic targets, has been extended to generalize its two parameters in terms of the electronic orbitals nl. The generalized MKLV (GKLV) with two sets of the species independent parameters for the same nl, one set for the ionization of inner orbits and another for the outermost orbit, is found profoundly successful in accounting for the EII cross section data of the K, L and M-shell neutral atoms with atomic numbers $Z = 1$–92 for the incident energies up to 1000 MeV in a consistent manner.

PACS. 34.80.Dp Atomic excitation and ionization by electron impact

1 Introduction

The interaction of an incident projectile with a target atom may give rise to different elastic and inelastic processes. Atomic ionization of is one of these processes, which are of fundamental importance for our understanding of collision dynamics. Furthermore, the knowledge of ionization cross sections is needed in numerous applied fields such as plasma physics, astrophysics, laser physics, semiconductor etching, radiation science, etc. The cross section data are also required in the quantitative elemental analyses using three types of material characterizations, e.g. electron probe microanalysis, Auger electron spectroscopy and electron energy loss spectroscopy. Thus, the electron impact ionization (EII) of atomic targets enjoys the heart of many applications in diverse fields.

Applications in modeling need a vast amount of sufficiently accurate EII cross sections (EIICS) for a wide range of atomic species and incident energies, as opposed to a few atomic targets and discrete incident energies, suitable for the measurement of EIICS data through experiments. The acute dearth of EIICS data calls for their theoretical determination. Various quantum mechanical methods, like Born approximations (BA) [1–3], coupled-channels approximations [4], and R-matrix methods [5] have been developed for accurate EIICS. These calculations, being arduous, cannot provide a speedy generation of the EIICS data for applications. Moreover, the rigorous calculations involve approximations and thus lead to limited applicability in terms of energy domain and species. This fact underscores the need for development of analytical empirical and semi-empirical models for rapid generation of EIICS data.

Good reviews of the simple-to-use models for EIICS data are given in [6,7]. The models, which have enjoyed wide applications, are the semi-classical models of Thomson [8], Gryzinski [9], and Kolbenstvedt [10], and the empirical formula of Lotz [11] and Bernshtam et al. [12]. The model of Deutsch and Märk (DM) [13] combines the binary-encounter approximation of Gryzinski with the dipole interaction of the Born-Bethe theory [14]. The binary-encounter-dipole (BED) model of Kim and Rudd [15] couples the modified form of Mott cross section [16] with the Born-Bethe theory [14]. BED requires the differential continuum oscillator strength (DOS) df/dw, which is difficult to find. The simplest approximate version of BED is the binary-encounter-Bethe (BEB) [15] model, which do not need the knowledge of DOS for calculation of EIICS. Uddin et al. [17] modified

[a] e-mail: uddinmda@yahoo.com

the BED model by incorporating ionic correction in it. While BED is adaptable to the neutral atoms and molecules, the modified BED (MBED) model is applicable to ionic targets with charge $q > 2$. Uddin et al. also incorporated ionic and relativistic ingredients in the simplified version of improved BED (iBED) model of Huo [18] to propound the modified relativistic iBED (MRIBED) [19–21]. The latter model has been found successful in describing EII for targets with atomic number $Z = 1$–92 in the hydrogen to beryllium sequences in a consistent way. Uddin group [22] also incorporated ionic and relativistic effects in the 6-parameter empirical model of Hombourger [23] and applied the modified Hombourger empirical model successfully to H and He-like targets with atomic numbers in the range $Z = 5$–92.

Recently, Haque et al. [24] incorporated the ionic and relativistic corrections to the empirical formula of Bell et al. (BELL) [25]. The parameters of the resulting modified BELL (MBELL), which have been generalized in terms of the ionizing orbitals and are independent of the species, are found abundantly successful in describing the EIICS data for the neutral and ionic targets, including the heavy ones, belonging to the K, L and M shells [24,26–28] over a wide range of incident energies up to 250 MeV. Although the MBELL model, to the best of our knowledge, appears to be the best performer, it is based on many fitting parameters.

The Kolbenstvedt (KLV) model [10,29] for calculating EIICS for the K-shell ionization of atoms is based on the sum of two contributions. The first one, σ_{ph}, stems from the distance collisions arising from an exchange of virtual photons between the incident electron and the target electrons leading to ionization by photoelectric effect. The second one, σ_M, is from the close collisions arising through the Møller interaction [30].

The KLV model, in its original form [10,29], has the drawback in that it unusually overestimates the cross sections from the threshold to peak region and underestimate them at ultra high energies. Uddin et al. [31] widened the applicability of the model to the K-shell ionization of atoms and ions at ultra-relativistic energies by modifying it with the following considerations:

(i) scaling down of σ_{ph} is effected through a multiplying factor F_M given by

$$\begin{aligned} F_M &= 2.5(1 - 1/U_{1s}) \quad \text{for} \quad U_{1s} \le 1.70, \\ &= 1.0 \qquad\qquad\quad \text{for} \quad U_{1s} > 1.70. \end{aligned} \tag{1}$$

Here, $U_{1s} = T/I_{1s}$ is the reduced energy with the incident energy T and the ionization energy I_{1s} for the $1s$ orbit (K-shell);

(ii) the correlation effect between the incident electron and target electrons in the form of shielding and ionic effects is taken care of by replacing the denominator $T(T+2)$ of σ_{ph} (see Eq. (5) below) with $T'(T'+1)$, T' being the effective kinetic energy given by

$$T' = T + \frac{\epsilon_{1s}(\chi_{1s} + I_{is})}{(q_{1s}+1)^{1/2}}. \tag{2}$$

Here, $q_{1s} = Z - 2$ is the effective charge [27] of the target as seen by the incident electron while ionizing the $1s$ orbit, except for H where $q_{1s} = 0$. $\epsilon_{1s} = 2$ is the ionic parameter for the K-shell. χ_{nl} is the kinetic energy of an electron in the K-shell;

(iii) the relativistic correction is effected through a factor R_F defined by

$$R_F = \left(1 + mU_{1s}^{\lambda}\right) \tag{3}$$

with $m = 0.054$ and $\lambda = 0.067$ [31].

In the modified KLV (MKLV) model of [31], the cross section for the K-shell ionization is given by

$$\sigma_{MKLV} = N_{1s} R_F \left(F_M \sigma_{ph} + \sigma_M\right). \tag{4}$$

Here, N_{1s} denotes the number of electrons in the K-shell. σ_{ph} and σ_M are given [31] by

$$\sigma_{ph} = \frac{0.141(T+1)^2}{I_{1s}T'_{1s}(T'_{1s}+2)} \times \left[\ln\frac{1.243(T+2)}{I_{1s}} - \frac{T(T+2)}{(T+1)^2}\right] \text{barns}, \tag{5}$$

and

$$\sigma_M = \frac{\eta_{1s}(T+1)^2}{I_{1s}T(T+2)} \times \left[1 - \frac{I_{1s}}{T}\left(1 - \frac{T^2}{2(T+1)^2} + \frac{2T+1}{(T+1)^2}\ln\frac{T}{I_{1s}}\right)\right] \text{barns}. \tag{6}$$

In equation (6), η_{1s} has the value $\eta_{1s} = 0.499$, such that $N_{1s}\eta_{1s} = 0.998$ with $N_{1s} = 2$ for the K-shell is the corrected value, following the classical electron radius $r_0 = 2.82 \times 10^{-15}$ m given in [29] to replace the factor $N_{1s}\eta_{1s} = 0.99$ in [10,31]. In equation (5), the factors $0.141N_{1s} = 0.282$ for the K-shell and 1.243 are the corrected values, for the same value of r_0, to replace, respectively, 0.275 and 1.19 in [10,31].

In the present work, we generalize expressions (1)–(6), for any ionizing orbit with orbital quantum numbers nl and take sum over all the ionizing orbits in (4) to obtain the total EIICS either in the considered shell or over all the shells of an atomic target. The generalized MKLV, henceforth referred to as GKLV, model is examined on the experimental EIICS data for the total ionization of H, He, Li, C, N. O, Mg, Si, P and S with the outermost orbit ranging from $1s$ to $3p$, as well as for the L-shell ionization of Ag, Sn, Ba, Ho, Ta, Au, Pb, Bi and U, and the M-shell ionization of Pb, Bi and U. In the subsequent discussion, the atoms with the respective outermost orbit in the K, L and M-shell are referred to as the K, L and M-shell atoms. To judge the performance of GKLV, we compare its results with those from our MBELL model [26–28] and the findings from available quantum mechanical calculations.

The paper is organized as follows. Section 2 provides the outline of the GKLV model. Section 3 deals with the presentation of results of analysis. A brief summary of conclusions is given in Section 4.

Table 1. Values of the parameters ϵ_{nl} and η_{nl} for the inner and outer shell ionization in the $1s$, $2s$, $3s$ and $3p$ orbits.

Parameter	Ionization	Orbits					
		$1s$	$2s$	$2p$	$3s$	$3p$	$3d$
ϵ_{nl}	Inner-shell†	2.00	1.00	1.00	2.00	0.30	0.1
	Outer-shell	2.50	2.00	2.00	0.50	1.50	–
η_{nl}	Inner-shell†	0.499	0.40	0.57	0.65	0.70	1.15
	Outer-shell	0.470	0.47	0.45	0.27	0.77	–

† Parameter values from [34] for the ionic targets.

2 Outline of the GKLV model

To generalize the expressions, the first one for the correlation and ionic corrections in (2) and the second one for the cross section σ_M arising from the Møller interaction in (6), we replace the quantities U_{1s}, I_{1s}, q_{1s}, ϵ_{1s} and η_{1s} in equations (1)–(6) by U_{nl}, I_{nl}, q_{nl}, ϵ_{nl} and η_{nl}, respectively, to make them dependent on nl. The total cross section in the generalized GKLV model, after summing the contributions over all ionized orbits, can be written as

$$\sigma_{GKLV} = \sum_{nl} N_{nl} R_F (F_M \sigma_{ph} + \sigma_M), \tag{7}$$

where, N_{nl} is the number of electrons in the ionizing nl orbit and the relativistic factor R_F is defined in (3). σ_{ph} and σ_M are now given by

$$\sigma_{ph} = \frac{0.141(T+1)^2}{I_{nl} T'_{nl}(T'_{nl}+2)} \times \left[\ln \frac{1.243(T+2)}{I_{nl}} - \frac{T(T+2)}{(T+1)^2}\right] \text{barns}, \tag{8}$$

and

$$\sigma_M = \frac{\eta_{nl}(T+1)^2}{I_{nl} T(T+2)} \times \left[1 - \frac{I_{nl}}{T}\left(1 - \frac{T^2}{2(T+1)^2} + \frac{2T+1}{(T+1)^2}\ln\frac{T}{I_{nl}}\right)\right] \text{barns}. \tag{9}$$

Here, the dependence of σ_{ph} in (8) on the parameter ϵ_{nl} comes through the effective kinetic energy T'_{nl}. η_{nl} is the second orbit dependent generalized parameter, involved in the expression of σ_M for the nl orbit.

3 Results and discussions

The ionization potentials I_{nl} are taken from Desclaux [32] and the kinetic energies χ_{nl} are calculated using the Dirac-Hartree-Fock code [33]. The parameters ϵ_{nl} and η_{nl} for the inner orbits are consecutively obtained from subsequent fitting of the EIICS data for $1s$, $2s$, $2p$ $3s$, $3p$ and $3d$ ionic targets [34]. The optimized parameter values, so obtained, are noted in Table 1.

The difference between an ion and a neutral atom lies only in the ionization cross section of the outer orbit. χ_{nl} is substantially lower for a neutral than the corresponding ion belonging to the same orbit. Thus, with the same value of ϵ_{nl}, T'_{nl} is significantly lower for a neutral atom leading to a misleading enhancement its EIICS over the ionic counterpart, as can be seen in equation (8). This enhancement of EIICS, in the case of neutrals, can be suppressed by a using larger value of parameter ϵ_{nl}, to balance the lower value of χ_{nl}, than the parameter for the ions. For the inner orbits, χ_{nl} and I_{nl} being similar in magnitudes for both ions and neutrals, χ_{nl} has to bear the same value for both types of targets.

The parameter values, deduced from from the ionic targets, are thus held fixed for the inner orbits of neutral targets. and also taken to serve as the starting values for their outermost orbit. The parameter ϵ_{nl} controls the peak position in addition to the magnitude of cross sections, while η_{nl} does for the magnitude only. The total effect of all ϵ_{nl}'s is to control the width of the overall peak and the η_{nl}'s to adjust the absolute cross sections. In fitting the EIICS data, ϵ_{nl} for the outermost orbit is adjusted first for the best overall width and position of the total peak. η_{nl} for the outermost orbit is then tuned to reproduce the absolute magnitude of EIICS at the peak position. The parameter values for the outermost orbits, as obtained in the present work, are also noted in Table 1. The large difference in the η_{nl} values for the inner and outermost orbits is not understood.

The sources of experimental EIICS data are Shah et al. [35] for H; Shah et al. [36], Schram et al. [37], Rejoub et al. [38], and Nagy et al. [39] for He; Zapesochnyl and Aleksakhin [40], McFarland and Kinney [41] and Jalin et al. [42] for Li; Brook et al. [43] for C, N and O; Fite and Brackmann [44] for O; Karstensen and Schneider [45,46] for Mg; and Freund et al. [47] for Mg, Si, P and S. The sources of available experimental EIICS data for the L-shell ionization are Hoffmann et al. [48] for Ag, Ta, Au, Pb, Bi and U; Ishii et al. [49] for Ag, Sn, Ba, Ho, Au, Pb, Bi and U; from Middleman et al. [50] for Ta, Au and Bi; from Reusch et al. [51] for Ta; and from Palinkas and Schlenk [52] for Au, Pb, Bi. For the M-shell ionization, the data are taken from Hoffmann et al. [48] for Pb, Bi and U, and from Ishii et al. [49] for Pb and Bi.

The GKLV results (solid lines) are compared with the total EIICS data in Figures 1 and 2. The GKLV predictions are also examined on the L- and M-shell ionization cross sections in Figures 3 and 4. To judge the comparative performance of the GKLV model, predictions from the DM model (dotted lines) using the parameter values given in [53], from the BEB model [15] (dashed lines),

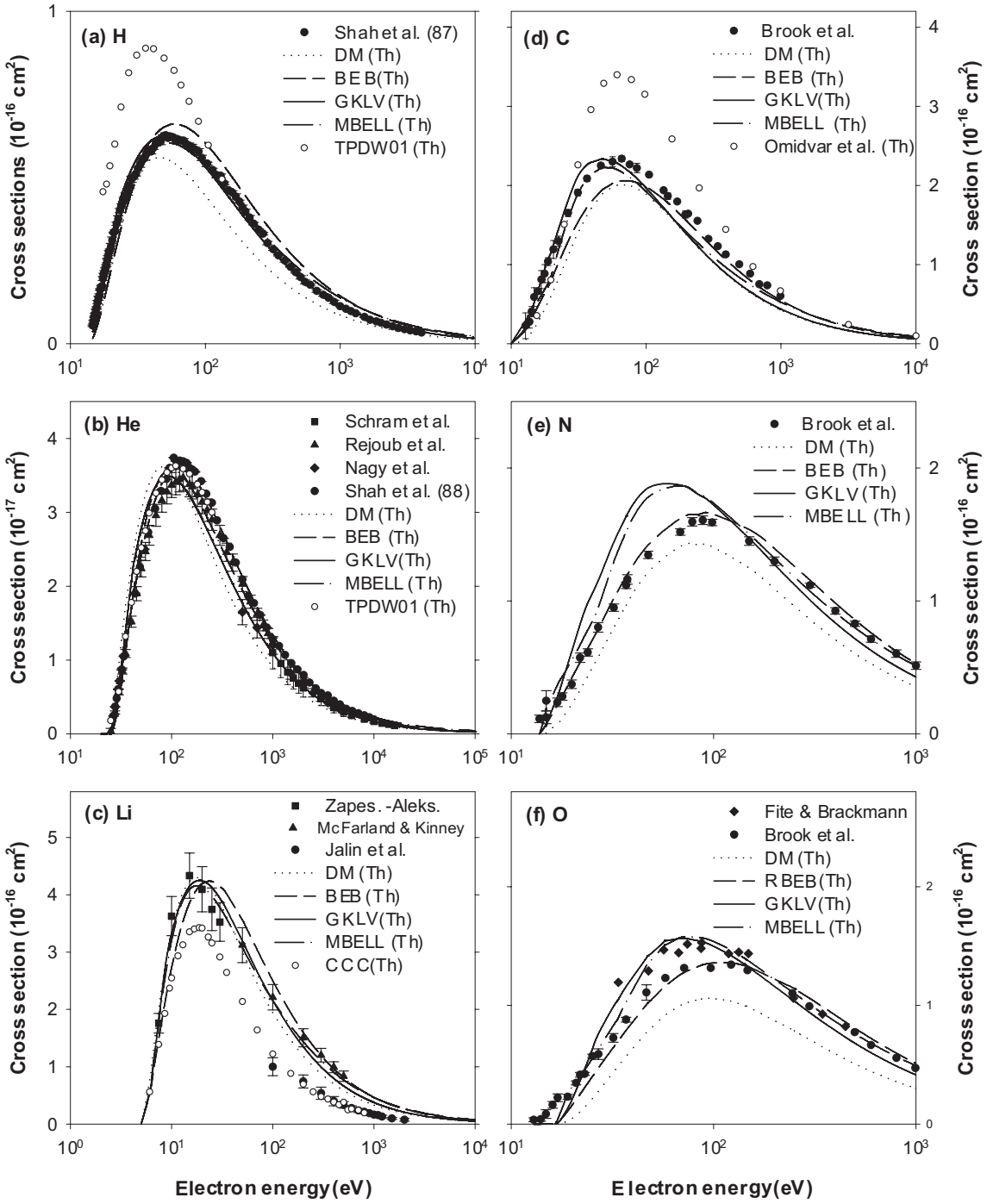

Fig. 1. Total EII cross sections of the K-shell atoms: (a) H and (b) He with $1s$ as the outer and the only ionizing orbit; and the L-shell atoms: (c) Li with $2s$ as the outer-orbit, and (d) C, (e) N and (f) O with $2p$ as the outer-orbit. The label Zapes.-Aleks. in (c) stands for the data of Zapesochnyl and Aleksakhin [40].

and the MBELL model (dash-dotted lines) using the parameters prescribed in [27,28] are also noted in the figures. To augment the comparative study, the relativistic two-potential distorted-wave Born approximation calculations (TPDW01) of Kuo and Huang [54] for H and He (Figs. 1a and 1b), the covergent-closed-coupling (CCC) predictions of Bray [55] for Li (Fig. 1c), the plane-wave Born approximation (PWBA) results of Omidvar et al. [56] for C (Fig. 1c), the PWBA cross sections of Khare and Wadehra [2] for the L and M-shell ionization of Ag, Ta, Au, Pb, Bi, U (Figs. 3 and 4), and the relativistic PWBA predictions of Scofield et al. [3] for the L-shell ionization of Ba, Ho, Au, Bi and U (Figs. 3 and 4) are also displayed.

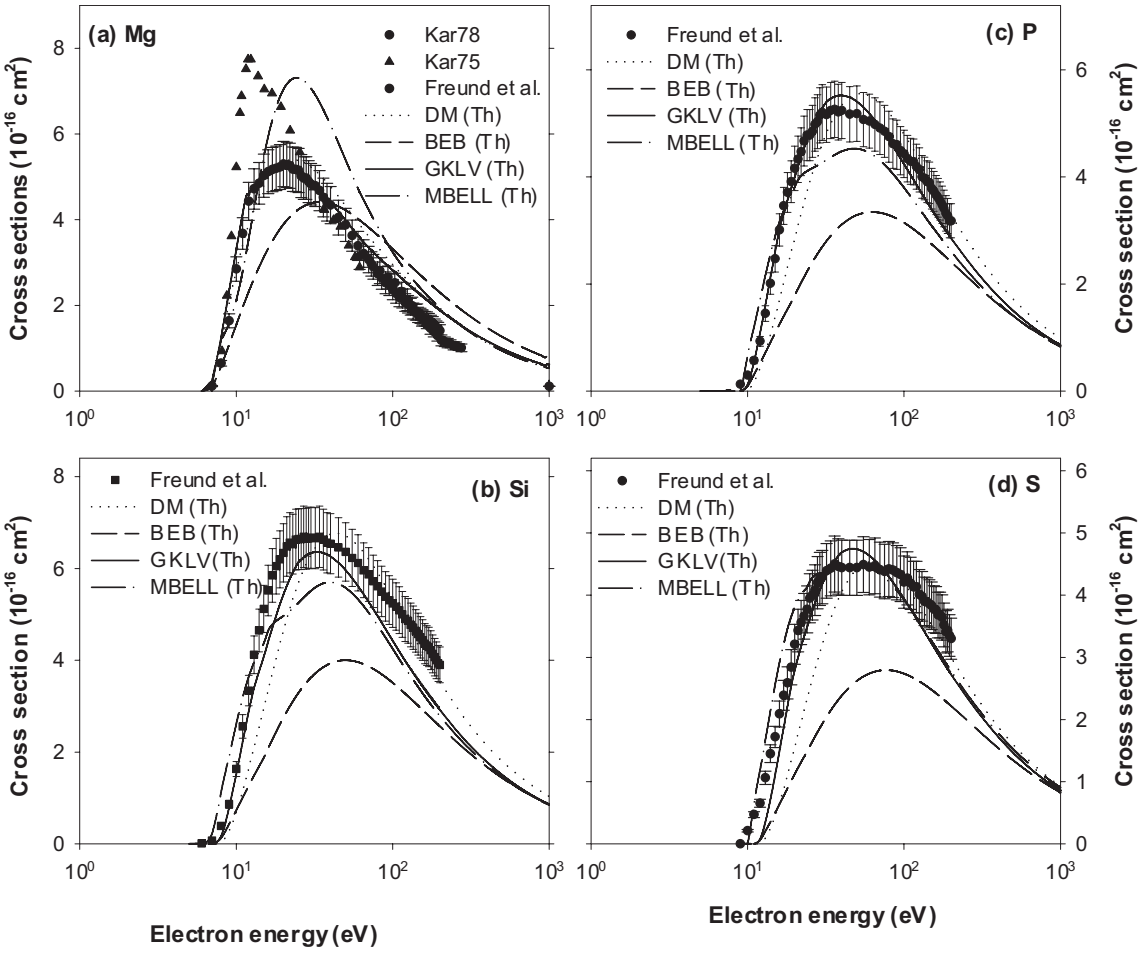

Fig. 2. Same as in Figure 1 for the M-shell atoms: (a) Mg with the outer-orbit as $3s$, and (b) Si, (c) P and (d) S with the outer-orbit being $3p$. The labels Kar75 and Kar78 in (a) denote the data of Karstensen and Schneider cited in [45,46], respectively.

The MKLV and MBELL models reproduce satisfactorily the EIICS data for all the atoms in the K, L, and M-shells, considered herein. BEB does best for the light atoms up to N (Fig. 1) and underestimate the cross sections for the M-shell atoms (Fig. 2), where DM perform better than BEB. The quantum mechanical TPDW01 calculation produces excellent fit to the data of He, although overestimates greatly the EIICS data of H around the peak region. The CCC calculations underestimate the data of Li and the PWBA predictions overestimate greatly the data of C around the peak region. The PWBA [2] and PDWBA [3] results (Figs. 3 and 4) for the L-shell ionization compare closely with the GKLV cross sections up to the ultra-relativisitc energies, where MBELL overestimates. However, the PWBA predictions of [2] and DM calculations for the M-shell ionization cross sections of Pb, Bi and U fail to reproduce the experimental data at energies in the range 10–1000 MeV, where both MKLV and MBELL work well. Judging from the fits to the total EIICS data for the M-shell atoms in Figure 2 and the L and M-shell ionization cross section data, the overall performance of the MKLV model is clearly the best among the models and ab initio methods considered herein.

4 Conclusions

The present work reports the performance of the generalized GKLV model, which accounts for well the EIICS data of K, L and M-shell atoms with the atomic number $Z = 1$–16 up to the 1 MeV incident energy and the L and M-shell ionization data of atomic targets with $Z = 47$–92 up to about 1000 MeV. The two sets of its generalized parameters ϵ_{nl} and η_{nl}, one for the ionization of inner orbits and another for the outermost orbit, are found to reproduce satisfactorily the total EIICS data of the K, L and M-shell atoms in a consistent manner. The same set of the parameters for the inner orbits reproduces the EIICS data for the L and M-shell ionization (Figs. 3 and 4) and has been found to describe successfully the EIICS data for the K-shell ionization of atoms and incident energies ions

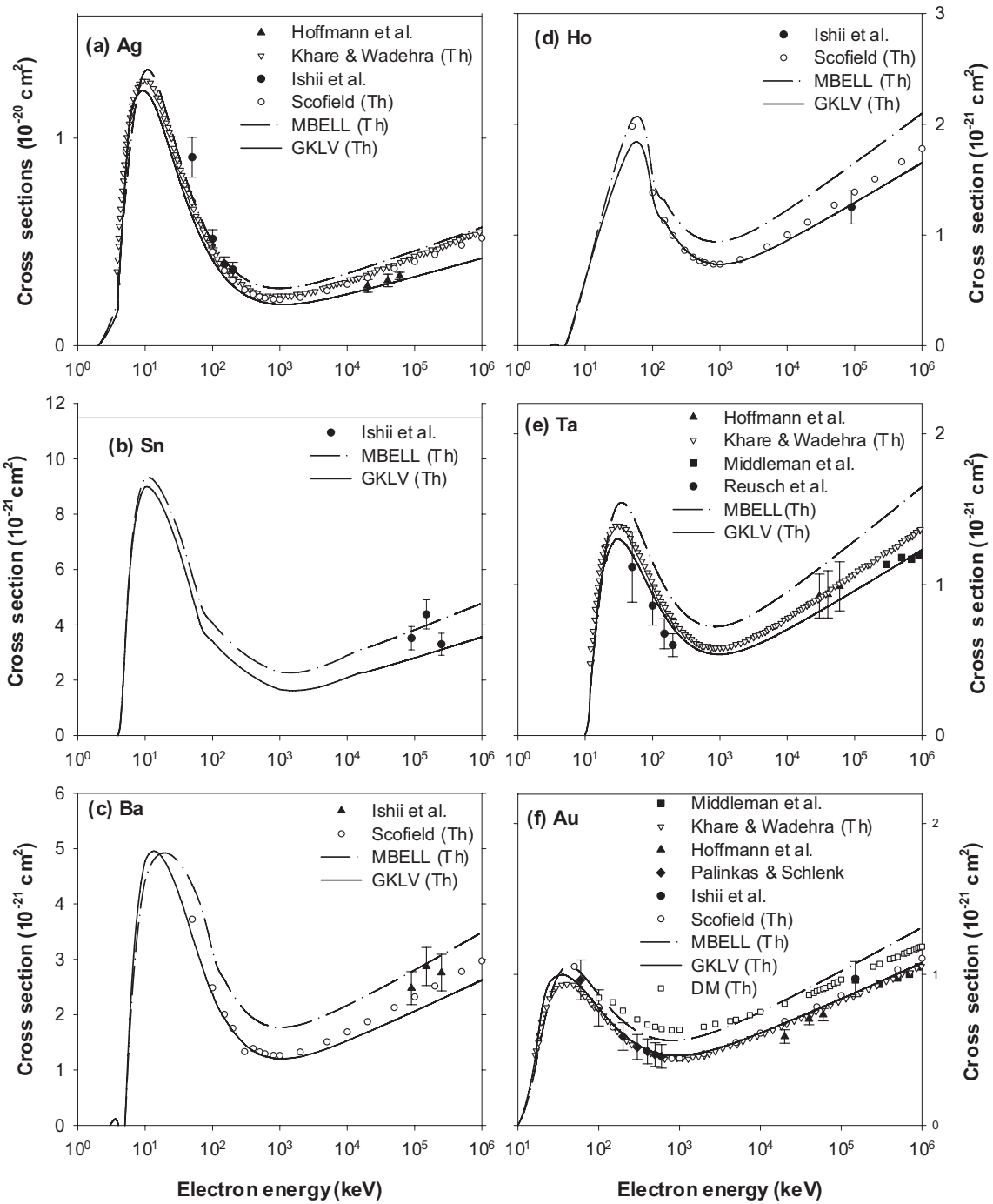

Fig. 3. EII cross sections of the L-shell ionization of (a) Ag, (b) Sn, (c) Ba, (d) Ho, (e) Ta and (e) Au. The sources of the experimental data are given in the text.

up to 10^4 MeV [31] and the total EIICS data for the L and M-shell ions up to 1 MeV [34].

The overall performance of the GKLV in describing the EIICS data of the neutral atoms from H to S is best among the widely used DM and BEB, and recently propounded MBELL models, and the ab initio theories considered herein. In particular, the GKLV model is remarkably good for the total ionization of M-shell atoms (Fig. 2), where the sophisticated quantum mechanical calculations are not available, and greatly successful in accounting for the M-shell ionization of heavy species like P, Bi and U in the incident energy range from about 20 to 2000 MeV, where ab initio methods fail (Fig. 4). MBELL overestimates the total ionization cross sections for Mg (Fig. 2a), the L-shell ionization cross section for Ho (Fig. 1d) and U (Fig. 2c), and underestimates the total EIICS for Si and P (Figs. 2b and 2c). The species independence of the two generalized parameters of the GKLV

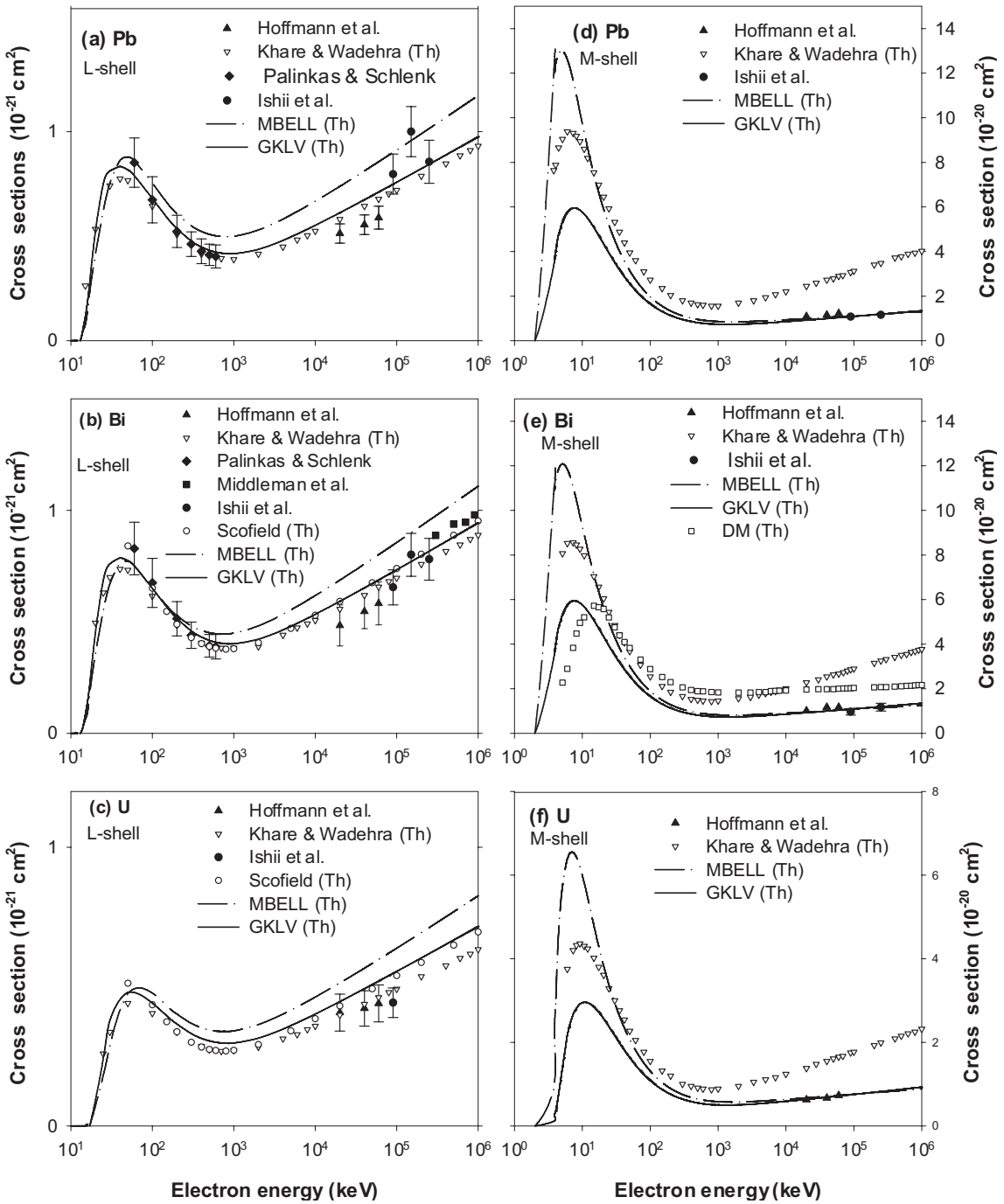

Fig. 4. EII cross sections of the L-shell ionization of (a) Pb, (b) Bi and (c) U, and M-shell ionization of (d) Pb, (e) Bi and (e) U. The sources of the experimental data are given in the text.

model, with its roots in quantum electrodynamics coupled with its profound success in describing the EIICS data of both ions and neutral atoms, lends it a complete model for quick generation of reliable EIICS data needed in modeling applications.

References

1. S.M. Younger, Phys. Rev. A **26**, 3177 (1982)
2. S.P. Khare, J.M. Wadehra, Can. J. Phys. **74**, 376 (1996)
3. J.H. Scofield, Phys. Rev. A **18**, 963 (1978)
4. I. Bray, A.T. Stelbovics, Adv. At. Mol. Opt. Phys. **35**, 209 (1995)
5. P. Burke, K. Berrington, *Atomic and molecular processes: An R-matrix Approach* (IOP Publishing, Bristol, 1993)
6. D.L. Moores, K.J. Reed, Adv. At. Mol. Opt. Phys. **34**, 301 (1994)
7. H. Deutsch, K. Becker, S. Matt, T.D. Märk, Int. J. Mass Spectrom. **197**, 37 (2000)
8. J.J. Thomson, Philos. Mag. Lond. **23**, 449 (1912)
9. M. Gryzinski, Phys. Rev. **138**, 336 (1965)

10. H. Kolbenstvedt, J. Appl. Phys. **38**, 4785 (1967)
11. W. Lotz, Z. Phys. **232**, 101 (1970)
12. V.A. Bernshtam, Y.V. Ralchenco, Y. Maron, J. Phys. B **33**, 5025 (2000)
13. H. Deutsch, T.D. Märk, Int. J. Mass Spectrom. Ion Process **79**, R1 (1987)
14. H. Bethe, Ann. Phys. (Lpz) **5**, 325 (1930)
15. Y.-K. Kim, M.E. Rudd, Phys. Rev. A **50**, 3954 (1994)
16. N.F. Mott, Proc. R. Soc. (Lond) A **126**, 259 (1930)
17. M.A. Uddin, A.K. Basak, A.K.M.A. Islam, F.B. Malik, J. Phys. B **37**, 1909 (2004)
18. W.M. Huo, Phys. Rev. A **64**, 042719 (2001)
19. M.A. Uddin, A.K.F. Haque, A.K. Basak, K.R. Karim, B.C. Saha, Phys. Rev. A **72**, 032715 (2005)
20. M.A. Uddin, A.K.F. Haque, M.M. Billah, A.K. Basak, K.R. Karim, B.C. Saha, Phys. Rev. A **71**, 032715 (2005)
21. M.A. Uddin, A.K.F. Haque, M.S. Mahbub, K.R. Karim, A.K. Basak, B.C. Saha, Int. J. Mass Spectrom. **244**, 76 (2005)
22. M.A. Uddin, A.K.F. Haque, K.R. Karim, A.K. Basak, Phys. Scripta **72**, 389 (2005)
23. C. Hombourger, J. Phys. B **31**, 3693 (1998)
24. A.K.F. Haque, M.A. Uddin, A.K. Basak, K.R. Karim, B.C. Saha, Phys. Rev. A **73**, 012708 (2006)
25. K.L. Bell, H.B. Gilbody, J.G. Hughes, A.E. Kingston, F.J. Smith, J. Phys. Chem. Ref. Data **12**, 891 (1983)
26. A.K.F. Haque, M.A. Uddin, A.K. Basak, K.R. Karim, B.C. Saha, F.B. Malik, Phys. Lett. A **354**, 449 (2006)
27. A.K.F. Haque, M.A. Uddin, A.K. Basak, K.R. Karim, B.C. Saha, F.B. Malik, Phys. Rev. A **73**, 052703 (2006)
28. A.K.F. Haque, M.A. Uddin, A.K. Basak, K.R. Karim, B.C. Saha, F.B. Malik, Phys. Scripta **74**, 377 (2006)
29. H. Kolbenstvedt, J. Appl. Phys. **46**, 2771 (1975)
30. C. Møller, Z. Phys. **70**, 786 (1931)
31. M.A. Uddin, A.K.F. Haque, K.R. Karim, A.K. Basak, F.B. Malik, Eur. Phys. J. D **37**, 361 (2006)
32. J.P. Desclaux, At. Data Nucl. Data Tables **12**, 325 (1973)
33. M.Y. Amusia, L.V. Chernysheva, *Computations of Atomic Processes* (Institute of Physics Publishing, Bristol, 1997)
34. A.K.F. Haque, M.A. Uddin, M.A.R. Patoary, A.K. Basak, K.R. Karim, B.C. Saha, F.B. Malik, unpublished
35. M.B. Shah, D.S. Elliott, H.B. Gilbody, J. Phys. B **20**, 3501 (1987)
36. M.B. Shah, D.S. Elliott, P. McCallion, H.B. Gilbody, J. Phys. B **21**, 2751 (1988)
37. B.L. Schram, A.J.H. Boerboom, J. Kistemaker, Physica **32**, 185 (1966)
38. R. Rejoub, B.G. Lindsay, R.F. Stebbings, Phys. Rev. A **65**, 042713 (2002)
39. P. Nagy, A. Skutlartz, V. Schmidt, J. Phys. B **13**, 1249 (1980)
40. I.P. Zapesochnyl, I.S. Aleksakhin, Sov. Phys. JETP **28**, 41 (1969)
41. R.H. McFarland, J.D. Kinney, Phys. Rev. **137**, A1058 (1965)
42. R. Jalin, R. Hagemann, R. Botter, J. Chem. Phys. **59**, 952 (1973)
43. E. Brook, M.F.A. Harrison, A.C.H. Smith, J. Phys. B **11**, 3115 (1978)
44. W.L. Fite, R.T. Brackmann, Phys. Rev. **113**, 815 (1959)
45. F. Karstensen, M. Schneider, Z. Phys. A **273**, 321 (1975)
46. F. Karstensen, M. Schneider, J. Phys. B **11**, 167 (1978)
47. R.S. Freund, R.C. Wetzel, R.J. Shul, T.R. Hayes, Phys. Rev. A **41**, 3575 (1990)
48. D.H.H. Hoffmann, C. Brendel, H. Genz, W. Low, S. Muller, A. Richter, Z. Phys. A **293**, 187 (1979)
49. K. Ishii, M. Kamiya, K. Sera, S. Morita, H. Tawara, M. Oyamada, T.C. Chu, Phys. Rev. A **15**, 906 (1977)
50. L.M. Middleman, R.L. Ford, R. Hofstadter, Phys. Rev. A **2**, 1429 (1970)
51. S. Reusch, H. Genz, W. Low, A. Richer, Z. Phys. D **3**, 379 (1986)
52. J. Palinkas, B. Schlenk, Z. Phys. A **297**, 29 (1980)
53. H. Deutsch, K. Becker, S. Matt, T.D. Märk, Int. J. Mass Spectrom. **197**, 17 (2000)
54. T.-Y. Kuo, K.-N. Huang, Phys. Rev. A **64**, 032710 (1995)
55. I. Bray, J. Phys. B **28**, L247 (1995)
56. K. Omidvar, H.L. Kyle, E.C. Sullivan, Phys. Rev. A **5**, 1174 (1972)